CRACK INITIATION AND MICROCRACK PROPAGATION UNDER CONSTANT AMPLITUDE AND PROGRAM LOADING HISTORIES

J. Foth*, H. Nowack*, G. Lütjering**

In the present study the initiation and propagation of small cracks was investigated. The propagation behavior of the small cracks is described on the basis of fracture mechanics. Under variable amplitude loading sequence effects occur, which can be quantitatively described by comparisons to linear damage calculations.

INTRODUCTION

Investigations of the formation and propagation of cracks at unnotched and notched specimens have shown that there are considerable differences between the actual test results and analytical predictions in many cases (1). An essential cause for the observed discrepancies is the definition of the crack initiation stage (2). Improvements of the prediction methods become only possible by more accurate evaluation of the microcrack formation and of the propagation behavior of the small cracks. Because the methods based on linear elastic fracture mechanics offer essential advantages for the description of the propagation behavior of fatigue cracks, it is of interest, if these methods can also be applied in the case of small cracks.

Specimens and components usually exhibit notches. That is the reason why the influence of stress raisers on the initiation of small cracks is of special interest.

Another most essential phenomenon from an engineering point of view is the fact that the accumulation of fatigue damage under variable amplitude loading is non-linear. The causes for the occurrence of the so-called load-sequence-effects is still not fully understood.

*Deutsche Forschungs- und Versuchsanstalt für Luft- und Raumfahrt (DFVLR), Institute of Materials Research, Fatigue Testing Branch, D-5000 Köln 90, Germany.

**Technische Universität , D-2000 Hamburg-Harburg, Germany

EXPERIMENTAL INVESTIGATIONS

The investigations of the initiation and propagation behavior of small cracks were performed on unnotched specimens with a square cross section and a K_t-value of about 1 as well as with plane specimens with double edge notches and a K_t-value of 3.3. The material was the technical aluminum alloy 2024-T3 (Cu = 4.4 %, Mg = 1.6 %, Zn = 0.25 %, Mn = 0.6 %, Fe = 0.5 %, Si = 0.5 %, others = 0.45 %, Al = Balance). For the observation of the initiation of small cracks at the unnotched specimens and at the notch surfaces, respectively, light-microscopes with a magnification of X100 - X1000 were used. At defined cycle numbers in the course of the tests all changes on the surfaces which had occurred were documented by a mapping procedure. The procedure enabled a detailed reconstruction of the crack initiation process at the end of the tests. Besides the mapping procedure photographs were made, as well. The photographs served as a basis for the SEM-analyses which were performed after the tests. Furtheron, investigations of the microstructural changes were performed in the TEM.

EXPERIMENTAL RESULTS

Based on the light-microscope investigation results the crack initiation and propagation process could be divided into four stages (3):

Stage I: Any cracks could be observed with the light-microscope.

Stage II: Microcracks were initiated and propagated independently.

Stage III: A transition from the microcracks to larger cracks by the coalescence of the individual cracks occurred. The cracks then propagated across the whole specimen surface.

Stage IV: The macrocrack became visible at the side surfaces of the specimens.

In Figure 1 the sum of the length of the individual small microcracks, which later form the macrocrack is plotted above the cycle number in the test. The SEM-analyses which were performed after the tests and which included Energy Dispersive X-ray Analyses showed, that the initiation of the cracks always occurred at the hard iron- and silicon-containing intermetallic phases. First the particles break due to slip processes in the aluminum matrix. After they have been broken in a direction perpendicular to the loading direction, the cracks propagate into the matrix material. The microscopic shape of the small cracks is roughly semi-circular or semi-elliptical.

For an analytical description of the extension of the semi-circular or semi-elliptical small cracks on the basis of linear elastic fracture mechanics, suitable calculation methods for the stress intensity factor have to be developed. A simple and efficient method is an alteration of a procedure which has first been proposed in (4). As it is shown in Figure 2 the stress intensity factor for the semi-elliptical crack in a notch, K_{NEC}, can be derived from the solutions for an elliptical crack in an unnotched specimen with a flat stress distribution, K_{EC} (5), which

is then multiplied by the relation K_{NLC}/K_{LC} to account for the influence of the stress gradient at the notch. The correction function for the stress intensity factor calculations for a notch containing a crack, K_{NLC}, is given in (6,7), and the K_{LC}-values for a plane specimen with double edge cracks are given in (8).

In Figure 3 the observed crack propagation behavior of all individual microcracks is plotted as a function of the variation in the stress intensity factor, for the unnotched specimen as well as for the double edge notched specimens. Also given is the basis-$da/dN=f(\Delta K)$-curve for the material investigated, which has been determined with specimens having long cracks. It can be seen that the propagation behavior of the individual cracks is given in its trend quite well. The influence of the interaction of the individual cracks and the coalescence of the cracks is not considered in the data.

Besides the investigation using constant amplitude loading, tests with non-constant amplitude loading histories were performed. In these tests so-called biharmonic load cycles were applied (9). These are complex cycles, where a cycle with a large load variation is always followed by a cycle with a smaller load variation. Applying the linear cumulative damage calculation method as it was proposed by Miner (10), a suitable basis for an evaluation of the non-linear damage accumulation under non-constant amplitude loading can be achieved. From the difference between the calculation and the behavior as it was observed in the actual test it can be seen how far the contribution to the damage due to the smaller load cycles is changed if they occur after cycles with a large load variation. In Figure 4 it can be seen that the damaging effect of the small load cycles is much larger within the biharmonic cycles than under constant amplitude loading with the amplitude and mean load of the small cycles. These load-sequence effects occurred mainly in the crack initiation stage rather than in the propagation stage of the small cracks. A main cause for the non-linear damage accumulation may be a non-linear slip mechanism acting under variable amplitude loading.

For a more detailed investigation of the crack propagation behavior under biharmonic loading the crack propagation rates as they were observed in the tests were also compared to a linear summation of the crack propagation rates under constant amplitude tests, which can be derived from the basis-$da/dN=f(\Delta K)$-curves with the adequate ΔK-values and at the instantaneous crack length (Figure 5).

If the trends are compared, which were observed in the comparison of the life behavior in the stages I, II, III and the linear damage calculation, on the one side, and in the comparison of the actual crack propagation rates in the stages II and III to the linearly calculated rates from the basis-$da/dN=f(\Delta K)$-curves, on the other side, there are indications that the sequence effects on the damage accumulation are somewhat more pronounced in stage I rather than in stage III.

SYMBOLS USED

a = extension of the (elliptical) surface cracks, smaller semi-axis of ellipse (mm)

c = extension of the (elliptical) surface cracks, greater semi-axis of ellipse (mm)

D = notch depth

da/dN = crack growth rate (m/cycle)

dc/dN = crack growth rate, surface cracks (m/cycle)

F = correction function for semi-elliptical cracks

G = correction function for a long crack in a notched specimen

ΔK = variation of the stress intensity factor ($MN \cdot m^{-3/2}$)

K_{EC} = stress intensity factor for a semi-elliptical surface crack in an unnotched specimen ($MN \cdot m^{-3/2}$)

K_{LC} = stress intensity factor for a through-the-thickness crack in an unnotched specimen ($MN \cdot m^{-3/2}$)

K_{NEC} = stress intensity factor for a semi-elliptical surface crack in a notched specimen ($MN \cdot m^{-3/2}$)

K_{NLC} = stress intensity factor for a through-the-thickness crack in a notched specimen ($MN \cdot m^{-3/2}$)

K_t = elastic stress concentration factor

l = crack length on the specimen/notch surface (mm)

N = cycle number

Q = shape correction function for semi-elliptical surface cracks

σ = remote stress ($MN \cdot m^{-2}$)

t = specimen thickness (mm)

W = specimen width (mm)

Y = correction function for the specimen geometry in stress intensity factor calculations

REFERENCES

1. Nowack, H., Hanschmann, D., Foth, J., Lütjering, G., and Jacoby, G., 1982, "Prediction Methods", ASTM-STP 770, Am. Soc. for Test. and Mats., to be published.

2. Hanschmann, D., 1981, DFVLR-FB81-10, DFVLR, Köln, Germany.

3. Foth, J., Nowack, H., and Lütjering, G., 1981, "Entstehung technischer Anrisse an Al 2024-T3 bei einstufigen und nicht-einstufigen Schwingbelastungen", Berichtsband DGM-Hauptversammlung Baden-Baden 1981, to be published.

4. Underwood, J.H., 1972, "Stress Intensity Factors for Internally Pressurized Thick-Wall Cylinders", ASTM-STP 513, Am. Soc. for Test. and Mats., 59.

5. Newman, J.C., Jr., 1979, "A Review and Assessment of the Stress-Intensity Factors for Surface Cracks", ASTM-STP 687, Am. Soc. for Test. and Mats., 16.

6. Tada, H., Paris, P.C., and Irwin, G.R., 1973, "The Stress Analysis of Cracks Handbook", Del Research Corp., St. Louis, Missouri.

7. Rooke, D.P., and Cartwright, D.J., 1976, "Compendium of Stress Intensity Factors", Her Majesty's Stationery Office, London, England.

8. Bowie, O.L., 1964, Journ. of Appl. Mech. 31, 208.

9. Nowack, H., 1971, DLR-FB 71-23, DFVLR, Köln, Germany.

10. Miner, M., 1945, "Cumulative Damage in Fatigue", Journ. of Appl. Mech., 159.

FIGURES

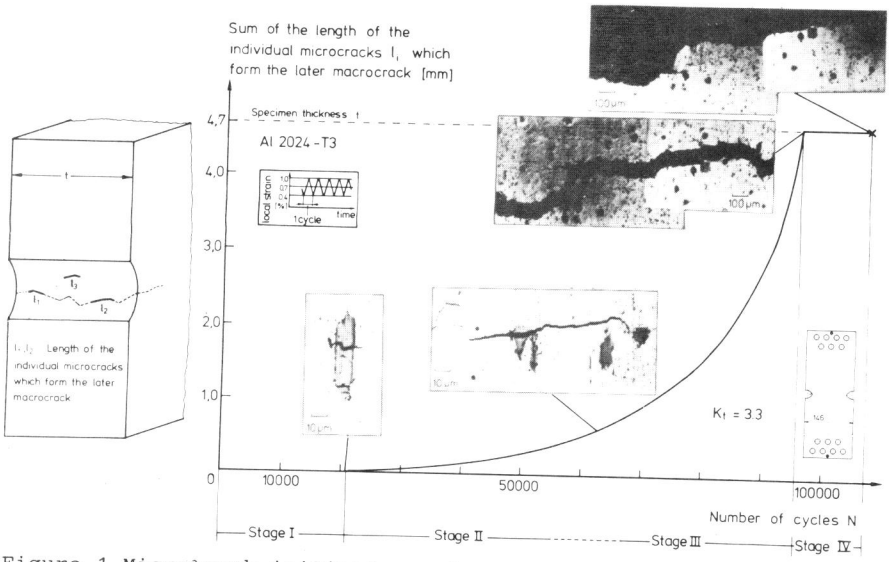

Figure 1 Microcrack initiation and propagation at the notch root

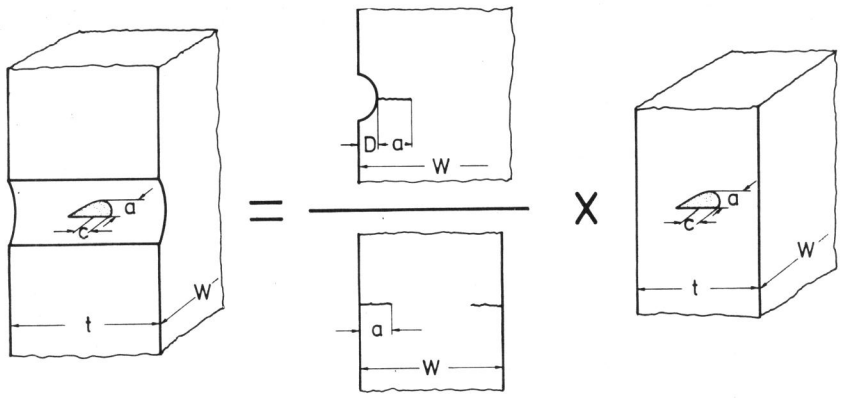

$$K_{NEC} = \frac{K_{NLC}}{K_{LC}} \times K_{EC}$$

$$K_{NLC} = \sigma \cdot \sqrt{\pi a} \cdot G$$
$$K_{LC} = \sigma \cdot \sqrt{\pi a} \cdot Y$$
$$K_{EC} = \sigma \cdot \sqrt{\frac{\pi a}{Q}} \cdot F$$

Figure 2 Estimation of the stress intensity factor

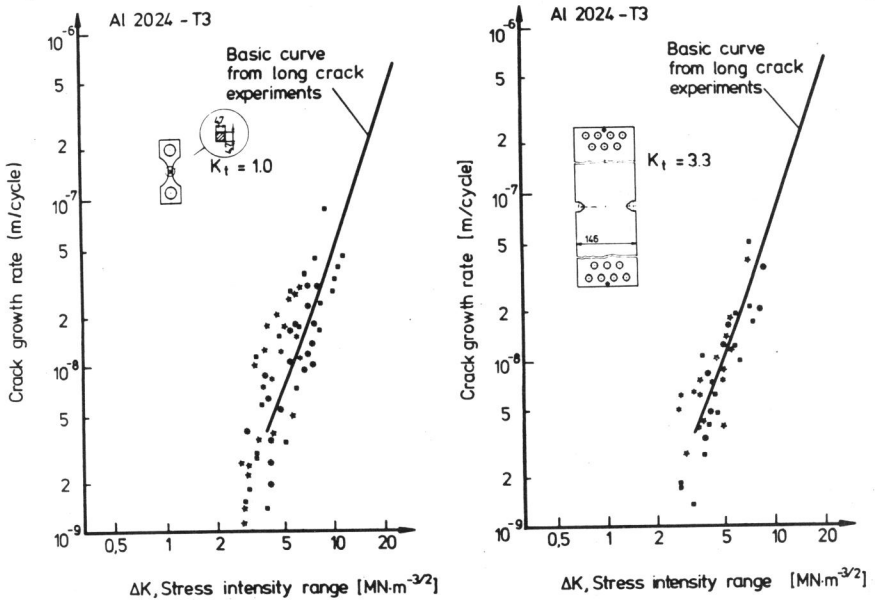

Figure 3 Microcrack growth

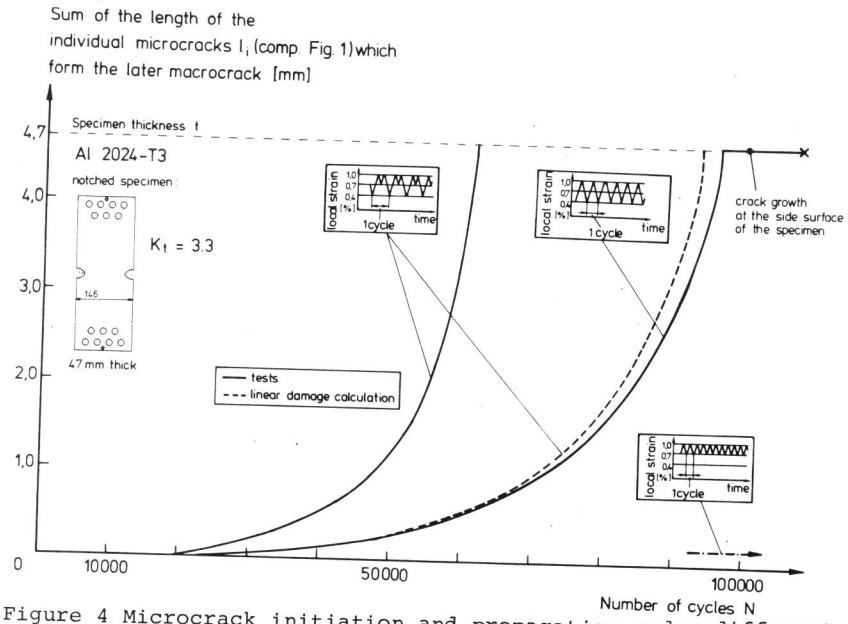

Figure 4 Microcrack initiation and propagation under different loading histories

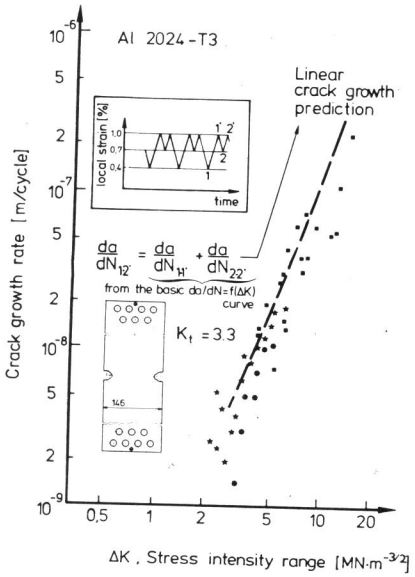

Figure 5 Microcrack growth under biharmonic loading history